

# Alteration of Oceanic Volcanic Glass: Textural Evidence of Microbial Activity

Martin R. Fisk, Stephen J. Giovannoni, Ingunn H. Thorseth

The subsurface biosphere may constitute as much as 50 percent of Earth's biomass. Direct and indirect evidence suggests that an extensive biosphere exists in the rocks below the sea floor. This survey of basalts of the Atlantic, Pacific, and Indian Oceans supports the hypothesis that bacteria have colonized much of the upper oceanic crust, which has a volume estimated at  $10^{18}$  cubic meters. Although this is the largest habitat on Earth, its low abundance of bacteria constitutes much less than 1 percent of Earth's biomass.

Microbes have been found living in sediments (1), sedimentary rocks (2), and volcanic rocks both on land (3) and in the oceans (4–6). Microbes and microbial products are abundant in oceanic hydrothermal vents and are presumed to be representatives of a community of thermophilic and hyperthermophilic microorganisms that is found below the sea floor (7, 8). Our previous studies (4–6, 9) support the hypothesis that microbes are involved in the transformation of minerals in the oceanic volcanic crust, in the extraction of elements from the crust, and in the deposition of elements in the crust. Thus, these microbes may have important geochemical roles. Here we present a survey of the range of conditions under which this presumed microbe-weathering association is found in the upper ocean crust.

The ocean crust is composed of sediment, basalt, and gabbro. The basalt includes a

jumble of erupted pillow lavas and sheet flows on top of near-vertical dikes, which are the conduits for the magma. Weathering of basalt by the circulation of seawater through the ocean crust results in the slow formation of secondary minerals from primary igneous minerals (feldspar, pyroxene, and olivine) and volcanic glass (formed when the 1200°C magma was quenched by cold seawater). This weathering, long thought to be solely a chemical process, is invariably found along fractures in the rocks and where voids between lava flows provide avenues for fluid flow. Chemical weathering of volcanic glass along a fracture in basalt is shown in Fig. 1A. Previous studies (4–6) of weathering of the quenched glass of ocean basalts have shown intricate weathering patterns and textures that are unlike the weathering that is produced by chemical weathering (Fig. 1A) or experimental alteration of glass (10). The intricate weathering textures were found to contain elevated amounts of carbon, phosphorus, and nitrogen relative to the glass, as well as traces of nucleic acids, which were indicated by fluorescent dyes (5, 6). In some cases, cell-like bodies were found in the weathered glass associated with these chemical signals (6).

To document the range of weathering textures and the range of conditions under which they formed, we examined several hundred basalt samples that were exposed on the sea floor and about 100 basalt samples that were buried from a few meters to 1.5 km below the sea floor (11). The basalts that we examined range from <1 million to 145 million years old; 10 samples are listed in Table 1.

The putative microbial weathering produced at least eight styles of pits, channels, tunnels, and voids (Fig. 1, B to H). These styles included irregular invasive fronts (Fig. 1B), smooth channels (Fig. 1, C and D), irregular branching channels (Fig. 1E), and string-of-bead shapes (Fig. 1F). Each channel style had a characteristic diameter, length, shape, and branching pattern. Channel diameters were 0.5 to 20  $\mu\text{m}$ , and lengths were from 1 to 200  $\mu\text{m}$ . Where channels branched, the channel and the branches were the same diameter (Fig. 1D). Different styles of morphologically distinct channels and pits were found in close association (Fig. 1C). Weathering was patchy (Fig. 1E) rather than evenly distributed (Fig. 1A). The channels were only seen in basalt that weathered at <100°C. Higher temperature weathering produced a smooth glass-clay interface (Fig. 1A). All of these observations are consistent with weathering facilitated by microbes.

Most channels and pits appeared to be either empty or filled with clay with no cells present, even when there was evidence of nucleic acids. We suggest that cells died, degraded, or lysed during or after sample collection. In a few cases, however, objects that may be the remnants of cells still remained in the channels. We observed three types: (i) individual 1- to 2- $\mu\text{m}$  spherical or oblong inclusions, spaced at intervals of 5 to 20  $\mu\text{m}$  along 2- $\mu\text{m}$ -diameter, smooth, long (100  $\mu\text{m}$ ) channels (Fig. 1, D and G); (ii) 8- $\mu\text{m}$ -diameter, cell-like inclusions, in smooth contorted channels; and (iii) 1- $\mu\text{m}$ -diameter filaments that ran the length of 100-

M. R. Fisk, College of Oceanic and Atmospheric Sciences, 104 Ocean Administration Building, Oregon State University, Corvallis, OR 97331-5503, USA. S. J. Giovannoni, Department of Microbiology, 220 Nash Hall, Oregon State University, Corvallis, OR 97331-3804, USA. I. H. Thorseth, Geological Institute, Allégaten 41, University of Bergen, 5007 Bergen, Norway.

**Table 1.** Conditions of microbial weathering. Latitude, longitude, water depth, sample depth, sediment thickness, in situ temperature, and age were measured during the Deep Sea Drilling Project and the Ocean Drilling Program. Dashes indicate sample not shown.

Sample	Area	Latitude	Longitude	Water depth (m)	Sample depth (m)	Sediment thickness (m)	In situ temperature (°C)	Age (Ma)	Figure
CD-1-6	Pacific Seamount	8°48'N	103°54'W	3300	0	0	2	3.5	1E
MR3-3R	Mendocino Ridge	40°22'N	127°16'W	1779	0	0	2	17	-
472-15-1-102	Pacific Seamount	23°00'N	113°60'W	2848	121	112	14	15	1F
482D-11-2-32	East Pacific Rise	22°47'N	107°59'W	3015	186	138	>100	0.4	1A
559-8-1-5	Mid-Atlantic Ridge	35°08'N	40°55'W	3754	292	238	8*	34	1B
561-1-2-30	Mid-Atlantic Ridge	34°47'N	39°02'W	3459	413	411	10*	19	1, C and D
713A-20-5-1	Chagos Ridge	4°12'S	73°34'E	2915	192	107	6*	45	-
765D-5-1-12	Argo Abyssal Plateau	15°59'S	117°35'E	5714	985	948	24	145	1, G and H
807C-92R-2-110	Ontong Java Plain	3°36'S	156°37'W	2806	1519	1380	61*	140	-
1026B-3R-1-45	Juan de Fuca Ridge	47°48'N	127°46'W	2658	268	229	61	3.5	-

\*Estimated on the basis of sample depth, a presumed thermal gradient of 2°C per 100 m, and 2°C bottom water.

## REPORTS

$\mu\text{m}$ -long, 2- $\mu\text{m}$ -diameter channels. Helical or septate channels (Fig. 1H) appeared in many of our samples; these morphologies are commonly associated with living cells.

Evidence supports the hypothesis that the unusual features that we describe here are of microbiological origin (5, 6). In particular, darkly stained tips of channels (Fig. 1H) coincide with the location of carbon, nitrogen, and phosphorus as determined by an electron microprobe; thus, the channel tips may contain degraded organic material (kerogen). Conclusive evidence that the diverse weathering patterns are the direct consequences of biological activity awaits analyses that identify the types of organisms associated with these phenomena and analyses that explain the role of these species in the weathering process.

We have not yet established which conditions correspond to the varied weathering textures shown in Fig. 1, but the depths of burial, the in situ temperatures, and the ages of 10 basalt samples are shown in Table 1. The in situ temperatures were measured during the Deep Sea Drilling Project and the Ocean Drilling Program, were inferred from heat flow in sea floor sediments that overlie the sample site, or were estimated on the basis of a thermal gradient of  $2^\circ\text{C}$  per 100 m. The alteration mineralogy of the basalt shows that some of our samples experienced oxidizing conditions (indicated by the presence of iron oxyhydroxides), whereas other samples experienced reducing conditions (indicated by iron sulfide). However, the oxidation state of most samples in Table 1 was not determined. The salinity of fluids below the sea floor can range from brines to fresher than seawater, and pH is typically  $<7$ ; however, salinity and pH have not yet been estimated for most of our samples. We also know little about the fluid flux through the basalt.

Although the physical and chemical conditions are not well known, we infer relations between basalt weathering and oxygen abundance and temperature. For example, sea floor surface samples rarely exhibited intricate weathering patterns. Perhaps cold, oxygenated bottom water is not a suitable medium for bacterial growth on or in basalt. Two rare examples of complex weathering of glass in sea floor surface basalts were found in samples CD-1-6 and MR3-3R (Table 1), but both samples could have been buried and later exposed by mass-wasting (CD-1-6) or by faulting (MR3-3R). On the other hand, all basalt samples that were buried by sediment and that contained glass exhibited some weathering similar to that shown in Fig. 1, B to H. Sediment seals the surface and reduces fluid flow, removes oxygen from fluids, and insulates the basalt, resulting in a gradual increase in temperature. A sediment depth of 100 m is sufficient to promote the intricate

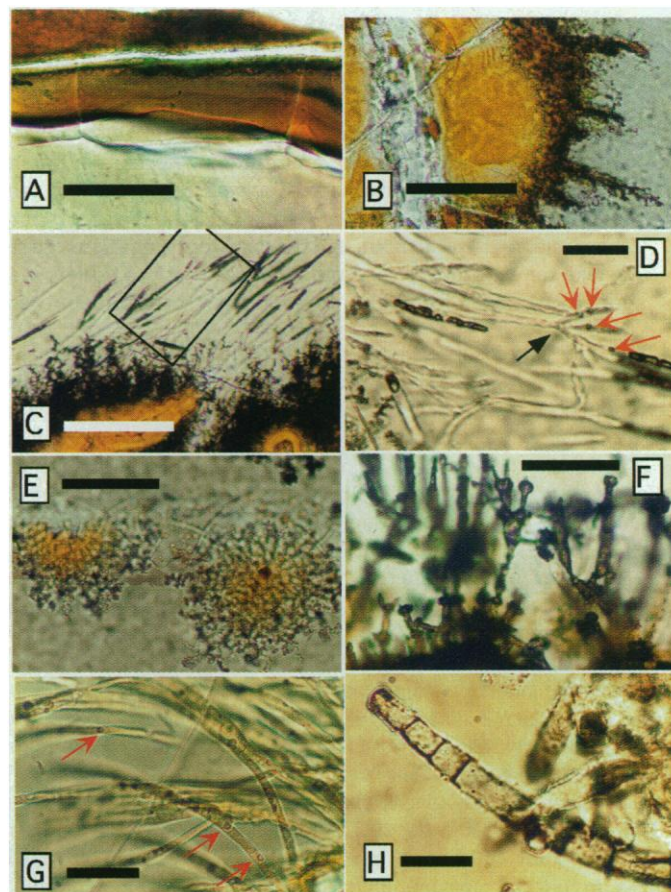
weathering textures (Fig. 1). Temperature may also have played a role in the types and the extent of weathering. The two samples with an in situ temperature of  $61^\circ\text{C}$  (Table 1) exhibit only one or two weathering styles and have channels that extend 50  $\mu\text{m}$  from fractures, whereas samples with in situ temperatures of between  $6^\circ$  and  $24^\circ\text{C}$  exhibit a wide variety of weathering styles and have channels that extend 200  $\mu\text{m}$  from fractures.

Although it has not been proven that microbes are responsible for the weathering of volcanic glass in the oceans, microbes could obtain metabolic energy or nutrients from the glass. Reduced iron, manganese, and sulfur are available as electron donors, and  $\text{Fe}^{3+}$  is available as an electron acceptor. Glass also contains small amounts of nutrients, such as phosphorus, and metals that could be used by microbes. Weathering of the rocks could also be an incidental

consequence of acids that are generated by the metabolism of organic carbon, hydrogen, or hydrogen sulfide in fluids that circulate in the ocean crust.

Microscopic examination and nucleic acid staining of volcanic glass indicate that the number of microorganisms in basalt is quite low and therefore not sufficient to produce snowblower vents with their abundant microbial floc (8). Organisms below the sea floor may undergo prolific growth at the time of magmatic intrusion because of increased permeability and higher heat flow. If we assume that there is 60 fg of C per cell and  $10^3$  cells per 1 g of glass (pillow basalts are about 2% glass), then the biological carbon in the oceanic crust is  $6 \times 10^{11}$  g, which is only a small fraction of the living carbon on Earth (about  $8 \times 10^{17}$  g of C). However, autotrophic microbes living on the chemical energy of Earth's volcanic rocks could also exist within

**Fig. 1.** Photomicrographs of altered glass margins of oceanic pillow basalts. All photomicrographs are of petrographic thin sections that are  $\sim 30 \mu\text{m}$  thick. Scale bars are 50  $\mu\text{m}$  for (A), (B), (C), (E), and (F). Scale bars are 10  $\mu\text{m}$  for (D), (G), and (H). (A) Reddish-brown clay surrounds a 10- $\mu\text{m}$ -wide open fracture (white) near the top of the panel. The clay replaces the yellowish-brown glass (bottom of panel) along a smooth alteration front that is typical of chemical weathering. The sample is from 12 km east of the East Pacific Rise (EPR) near the Tamayo fracture zone. (B) A fracture through glass (left) is surrounded by reddish-brown clay. Fresh glass (gray) is at the right of the panel. The glass-clay boundary is irregular and dark brown to black. Channels (10  $\mu\text{m}$  wide and 20 to 60  $\mu\text{m}$  long) extending from the clay into the glass are terminated with 1- $\mu\text{m}$ -diameter channels. Irregular glass-clay interfaces (as shown here) contain nucleic acids, carbon, and phosphorus (5, 6). (C) Orange-brown clay replaces glass in the bottom of the panel, and glass is present across the top. The glass-clay boundary is dark and irregular [similar to (B)]. A second style of channel (100  $\mu\text{m}$  long, 2 to 4  $\mu\text{m}$  wide) extends deep into the glass. The box indicates the location of (D). (D) Detail of (C), showing the branching channel (black arrow) and the cell-sized objects in the channels (red arrows). (E) A thin fracture ( $\sim 1 \mu\text{m}$ ) runs across the middle of the panel, along which are centered radiating, irregular, branching channels that extend 20  $\mu\text{m}$  from the clay-glass boundary. The sample is from the EPR off-axis seamount. (F) Irregular, bulbous channels that are  $\sim 5 \mu\text{m}$  in diameter and 50  $\mu\text{m}$  in length invade the glass from the clay-glass boundary. (G) Channels contain round or oblong (about 1  $\mu\text{m}$  in diameter) objects that are spaced every 5 to 20  $\mu\text{m}$  (red arrows). (H) Same sample as (G). The channel has septate divisions and a darkly stained tip.



other planetary bodies where fluid flow establishes gradients in redox potential, as long as there are sources of required nutrients, water, and carbon.

## References and Notes

1. R. J. Parkes *et al.*, *Nature* **371**, 410 (1994).
2. D. R. Lovely and F. H. Chapelle, *Rev. Geophys.* **33**, 365 (1995); S. V. Liu *et al.*, *Science* **277**, 1106 (1997); C. Zhang *et al.*, *Geochim Cosmochim. Acta* **61**, 4621 (1997).
3. T. O. Stevens and J. P. McKinley, *Science* **270**, 450 (1995); I. H. Thorseth, H. Furnes, M. Heldal, *Geochim. Cosmochim. Acta* **56**, 845 (1992).
4. I. H. Thorseth, I. Torsvik, H. Furnes, K. Muehlenbachs, *Chem. Geol.* **126**, 137 (1995); H. Furnes, I. Thorseth, O. Tumyr, T. Torsvik, M. Fisk, *Proc. Ocean Drill. Program Sci. Results* **148**, 191 (1996); S. J. Giovannoni, M. R. Fisk, T. D. Mullins, H. Furnes, *ibid.*, p. 207.
5. T. Torsvik, H. Furnes, K. Muehlenbachs, I. H. Thorseth, O. Tumyr, *Earth Planet. Sci. Lett.*, in press; M. R. Fisk, S. J. Giovannoni, T. D. Mullins *Eos (Fall Meet. Suppl.)* **75**, 706 (1994).
6. M. R. Fisk, S. J. Giovannoni, E. Urbach, I. H. Thorseth, *Eos (Fall Meet. Suppl.)* **78**, 740 (1997).
7. R. Huber, P. Stoffers, J. L. Cheminee, H. H. Richnow, K. O. Stetter, *Nature* **345**, 179 (1990).
8. R. M. Haymon *et al.*, *Earth Planet. Sci. Lett.* **119**, 85 (1993); S. K. Juniper, P. Martineau, J. Sarrazin, J. Y. Gélinais, *Geophys. Res. Lett.* **22**, 179 (1995); C. D. Taylor and C. O. Wirsen, *Science* **277**, 1483 (1997).
9. I. H. Thorseth, H. Furnes, O. Tumyr, *Chem. Geol.* **119**, 139 (1995).
10. J. L. Crovisier, J. Honnorez, J. P. Eberhart, *Geochim. Cosmochim. Acta* **51**, 2977 (1987); G. Berger, C. Claparols, C. Guy, V. Daux, *ibid.* **58**, 4875 (1994).
11. Sea floor surface samples were collected by dredges and submersibles from seamounts and mid-ocean ridges. Buried samples were collected during the Deep Sea Drilling Project and the Ocean Drilling Program.
12. NSF and the Joint Oceanographic Institutions supported this work. Samples are from the Ocean Drilling Program sample repositories and from D. Graham, D. Christie, R. Embley, and M. Perfit. The photomicrographs were taken with Nikon and Leica microscopes, which were loaned by D. Graham and F. Moore.

9 March 1998; accepted 30 June 1998

## A 3000-Year Climatic Record from Biogenic Silica Oxygen Isotopes in an Equatorial High-Altitude Lake

M. Rietti-Shati, A. Shemesh,\* W. Karlen

A record of oxygen isotopes in biogenic opal, 4200 to 1200 calibrated years before the present, from a high-altitude proglacial lake on Mount Kenya, East Africa, exhibits short-term fluctuations on a time scale of centuries as well as long-term variations. The short-term fluctuations are attributed to changes in the glacier meltwater input, and the long-term variations are related to changes in lake temperature. The record indicates that the climate was warm in Equatorial East Africa from 2300 to 1500 years before the present.

The Holocene, although relatively more stable than the Late Pleistocene, was also subject to abrupt climatic changes (1, 2). Small, low-latitude glaciers are especially sensitive to such climatic changes (3). Mount Kenya, in East Africa, is a dormant volcano that contains several small glaciers and lakes located at an elevation of 4200 to 5200 m (Fig. 1). In 1978 two ice cores were retrieved from the col (4870 m) between the Lewis and Gregory glaciers on Mount Kenya (Fig. 1). However, the lack of a clear relation between air temperature and the isotopic composition of the ice hampered detection of climatic signals (4). Karlen and Rosqvist (5) investigated the sediments from Hausberg Tarn, a proglacial lake, to study glacier fluctuations on Mount Kenya (0°10'S 37°20'E; Fig. 1). X-ray radiography of the cores, together with changes in organic content, indicates that there has been a succession of glacier advances and retreats during the past 4000 years (5). These findings are qualitative because the

high-altitude lakes in East Africa are void of the carbonate material (6) that is commonly used for isotopic studies of climate change. On the other hand, these lakes contain biogenic opal that is suitable for isotopic analysis. Here we report oxygen isotope measurements of biogenic opal from Hausberg Tarn.

The climate of East Africa is affected by the seasonal position of the intertropical convergence zone and regional factors associated with lakes, topography, and maritime influence (7). The lower tropospheric flow over East Africa comes predominantly from the southeast, and, because of the topographic control, maximum rainfall occurs at intermediate elevations (2500 to 3000 m) on the southern and eastern flanks of Mount Kenya (5). Above 4500 m, most of the annual precipitation (700 to 800 mm) falls as snow. Temperatures average about 0°C (4, 5) and are lowest in March and April and highest in July and August.

We obtained a 180-cm-long sediment core from Hausberg Tarn in 1996 (Fig. 1). The top part of the core, containing the most recent sediment was too soft, and could not be retrieved by our coring device. The lake (area, 12,000 m<sup>2</sup>; 10 m at the deepest part) is located near the moraines of Cesar and Joseph Glaciers (Fig. 1) and its sediments contain both authi-

genic opal produced by diatoms and allochthonous material derived from the surrounding steep mountain slopes (5). Diatoms are photosynthetic algae that secrete opal (SiO<sub>2</sub>·nH<sub>2</sub>O) as an internal shell with a known isotopic fractionation between the opal and the water. The temperature dependency of the opal-water fractionation is given by

$$t^{\circ}\text{C} = 11.02 - 2.04(\delta^{18}\text{O}_{\text{si}} - \delta^{18}\text{O}_{\text{w}} - 40) \quad (1)$$

where  $t$  is the water temperature and  $\delta^{18}\text{O}_{\text{si}}$  and  $\delta^{18}\text{O}_{\text{w}}$  are the isotopic compositions of opal and water, respectively (8–11). Thus, the measurement of  $\delta^{18}\text{O}_{\text{si}}$  provides information both about the lake temperature and about the  $\delta^{18}\text{O}_{\text{w}}$  of the lake in the past (12).

In 1997 we analyzed water samples from the lake, from surrounding streams, and from rainwater collected at Mackinder camp (located at an altitude of 4200 m) to determine the composition of the water flowing to the lake today. The isotopic composition of all water samples was measured by standard techniques for  $\delta^{18}\text{O}$  and  $\delta^2\text{H}$ . Eight <sup>14</sup>C accelerator mass spectrometry dates on bulk organic matter of the core (13) indicate that the average sediment accumulation was 0.62 mm/year (Fig. 2A).

The  $\delta^{18}\text{O}$  values of the lake's surface and deep water are both  $-6.3$  per mil and indicate that the lake is not stratified. Therefore, diatom  $\delta^{18}\text{O}_{\text{si}}$  values represent the whole water volume despite the fact that most of the fossil diatoms are bottom dwellers. Although Hausberg Tarn has an outlet to Oblong Tarn (Fig. 1), whose  $\delta^{18}\text{O}_{\text{w}}$  value is  $-6.4$  per mil, it has no visible inlet. The lake  $\delta^{18}\text{O}_{\text{w}}$  is similar to the  $\delta^{18}\text{O}_{\text{w}}$  value of the Lewis Glacier meltwater stream ( $-6.2$  per mil) and also to the overall average  $\delta^{18}\text{O}$  of the Lewis Glacier ice cores (4) (10-m-long cores). Because of their geographic proximity and similar altitude (Fig. 1), we assume that the Cesar and Josef Glaciers have  $\delta^{18}\text{O}$  values similar to that of the Lewis Glacier. The rainwater  $\delta^{18}\text{O}_{\text{w}}$  values obtained from Mackinder camp (4200 m) are  $-0.6$  and  $-1.4$  per mil. Thus, we conclude that Hausberg Tarn is a through-flow

M. Rietti-Shati and A. Shemesh, Department of Environmental Sciences and Energy Research, Weizmann Institute of Science, Rehovot 76100, Israel. W. Karlen, Department of Physical Geography, University of Stockholm, Stockholm S-106 91, Sweden.

\*To whom correspondence should be addressed.